Glycobiology vol. 24 no. 9 pp. 852–863, 2014
doi:10.1093/glycob/cwu047
Advance Access publication on May 23, 2014

Glyco-variant library of the versatile enzyme horseradish peroxidase

Simona Capone[2], Robert Pletzenauer[2], Daniel Maresch[3], Karl Metzger[2], Friedrich Altmann[3], Christoph Herwig[2], and Oliver Spadiut[1,2]

[2]Institute of Chemical Engineering, Research Area Biochemical Engineering, Vienna University of Technology, Vienna 1060, Austria and [3]Department of Chemistry, University of Natural Resources and Life Sciences, Vienna 1190, Austria

Received on April 11, 2014; revised on May 20, 2014; accepted on May 20, 2014

When the glycosylated plant enzyme horseradish peroxidase (HRP) is conjugated to specific antibodies, it presents a powerful tool for medical applications. The isolation and purification of this enzyme from plant is difficult and only gives low yields. However, HRP recombinantly produced in the yeast *Pichia pastoris* experiences hyperglycosylation, which impedes the use of this enzyme in medicine. Enzymatic and chemical deglycosylation are cost intensive and cumbersome and hitherto existing *P. pastoris* strain engineering approaches with the goal to avoid hyperglycosylation only resulted in physiologically impaired yeast strains not useful for protein production processes. Thus, the last resort to obtain less glycosylated recombinant HRP from *P. pastoris* is to engineer the enzyme itself. In the present study, we mutated all the eight N-glycosylation sites of HRP C1A. After determination of the most suitable mutation at each N-glycosylation site, we physiologically characterized the respective *P. pastoris* strains in the bioreactor and purified the produced HRP C1A glyco-variants. The biochemical characterization of the enzyme variants revealed great differences in catalytic activity and stability and allowed the combination of the most promising mutations to potentially give an unglycosylated, active HRP C1A variant useful for medical applications. Interestingly, site-directed mutagenesis proved to be a valuable strategy not only to reduce the overall glycan content of the recombinant enzyme but also to improve catalytic activity and stability. In the present study, we performed an integrated bioprocess covering strain generation, bioreactor cultivations, downstream processing and product characterization and present the biochemical data of the HRP glyco-library.

Keywords: bioprocess technology / glyco-engineering / glycosylation / horseradish peroxidase / *Pichia pastoris*

Introduction

The heme-containing plant enzyme horseradish peroxidase (HRP; EC 1.11.1.7) is a Class III peroxidase catalyzing the oxidation of various substrates (e.g., amines, aromatic phenols, indoles, phenolic acids and sulfonates) using hydrogen peroxide (H_2O_2) as oxidant. Horseradish peroxidase exists in at least 19 different isoenzyme forms in the horseradish root (*Armoracia rusticana*), of which isoenzyme C1A is the most abundant and thus the most studied one (e.g., Dunford 1999; Veitch and Smith 2001; Veitch 2004; Carlsson et al. 2005; Krainer et al. 2013; Spadiut and Herwig 2013). It is a 34 kDa monomeric oxidoreductase containing a heme-group as well as two Ca^{2+}-ions as prosthetic groups. The crystal structure of HRP C1A led to the identification of nine N-glycosylation sites of the Asn-X-Ser/Thr type, where X can be any amino acid but proline, of which eight are occupied when the enzyme is expressed in plant (Smith et al. 1990), which is why the molecular mass of HRP C1A increases from 34 to ~44 kDa (Veitch 2004; Spadiut and Herwig 2013). Due to glycosylation and the presence of both, the heme-group and disulfide bridges, the recombinant production and subsequent preparative purification of HRP has proven to be very difficult (Smith et al. 1990; Gajhede et al. 1997; Lavery et al. 2010; Spadiut et al. 2012), which is why HRP is still mainly isolated from plant (Lavery et al. 2010). However, HRP preparations from plant describe a mixture of isoenzymes, which seasonally varies in composition and concentration, and yields are extremely low (Jermyn 1952; Jermyn and Thomas 1954; Shannon et al. 1966). Since HRP is a versatile enzyme used in numerous, quite diverse industrial and medical applications, such as waste water treatment, fine chemical synthesis, immunoassays, biosensors and coupled enzyme assays (e.g., Krieg and Halbhuber 2003), the controllable recombinant production and subsequent efficient purification of single HRP isoenzymes is highly desired. Thus, we have not only investigated and improved the recombinant production of the isoenzyme HRP C1A with *Pichia pastoris* in the past few years (Dietzsch et al. 2011a,b; Krainer et al. 2012; Zalai et al. 2012; Spadiut et al. 2013), but also developed an efficient downstream process for the hypermannosylated enzyme recombinantly derived from this yeast (Spadiut et al. 2012; Krainer, Pletzenauer, et al. 2013). However, for medical applications where HRP is conjugated to antibodies, like antibody-directed enzyme-prodrug therapy (Folkes and Wardman 2001; Wardman 2002) and medical

[1]To whom correspondence should be addressed: Tel: +43-1-58801-166473, Fax: +43-1-58801-166980, e-mail: oliver.spadiut@tuwien.ac.at

diagnostics (Romero et al. 1999; Huang 2001; Palmgren et al. 2011; Dotsikas and Loukas 2012), the degree of glycosylation of HRP is of utmost importance, since not only the stability of the enzyme but also the conjugation with antibodies is expected to change with varying glycosylation. Besides, the untrimmed yeast-derived high-mannose containing glycosylation can trigger immune responses in humans (personal communication with Dr. Lisa Folkes; Gray Institute for Radiation Oncology and Biology, Department of Oncology, University of Oxford).

Obviously, the availability of an enzyme without or at least with reduced surface glycosylation would solve abovementioned problems. However, the biological role and importance of glycans for plant peroxidases is still not completely understood and is topic of numerous studies in glycobiology. So far, some studies report stabilizing effects of the glycans (Narhi et al. 1991; Wang et al. 1996), whereas other studies do not show such effects (Ehlers et al. 1992; Powell and Pain 1992). In 1990, Smith et al. (1990) were able to produce active and correctly folded HRP without any glycans in *Escherichia coli*. In a following study, Tams and Welinder analyzed the importance of the glycosylation for HRP in more detail (Tams and Welinder 1998). They showed that the removal of most of the glycans, except the *N*-acetylglucosamine residues, by a mild chemical deglycosylation with trifluoromethanesulfonic acid resulted in a fully active, but less stable enzyme (Tams and Welinder 1995, 1998). Both studies showed that glycans on the surface of HRP affect the physicochemical properties of the enzyme but are not required for catalytic activity. However, chemical deglycosylation only left 60% of HRP active and also describes a quite cumbersome procedure (Tams and Welinder 1995, 1998), which is why it is not a useful method to obtain unglycosylated HRP. Although recombinant proteins from *P. pastoris* can also be deglycosylated enzymatically (Sainz-Pastor et al. 2006; Kang et al. 2012), also this option has to be reconsidered, since (1) enzymatic deglycosylation is only quantitative when the target protein is denatured and (2) the additional endoglycosidases have to be removed again to obtain pure product. Another way to control and reduce the complexity of native yeast-like glycosylation on glycoproteins secreted from *P. pastoris* is through glyco-engineering (Choi et al. 2003; Hamilton et al. 2003; Vervecken et al. 2004; Hamilton and Gerngross 2007). A key event in such engineering is the knockout of the OCH1 gene, which initiates outer-chain elongation, leading to hypermannosylation. However, in a previous study, where we knocked out this gene, we observed that HRP with reduced glycan complexity possessed hampered downstream processing and that the glyco-engineered *P. pastoris* strains generated were physiologically impaired, impeding efficient production processes (Krainer et al. 2013).

Consequently, the last resort to efficiently produce HRP with a reduced amount of surface glycosylation is to glyco-engineer the enzyme itself. In a recent study, two selected Asn residues of HRP were mutated to Asp to analyze effects on the stability of the enzyme and to produce more properly folded HRP in *E. coli* (Asad, Khajeh, et al. 2011). Asad, Khajeh, et al. (2011) showed that introducing the mutations Asn13Asp and Asn268Asp did not just affect the production of HRP in *E. coli*, but also increased the catalytic constants as well as the thermal stability. These results did not only underline the possibility of obtaining active and correctly folded HRP with reduced glycosylation but also showed that mutating the glycosylation sites may even have beneficial effects on catalytic activity and stability.

In the present study, we generated a glyco-variant library of HRP C1A exchanging all the eight Asn serving as glycosylation sites by the structurally similar amino acids Asp, Gln or Ser. We did not only investigate the effects of the single mutations on enzyme activity and stability but also on protein purification following an integrated bioprocess technology approach. After determining the most suitable mutation at the single N-glycosylation sites, we physiologically characterized the respective *P. pastoris* strains in the controlled environment of a bioreactor. A two-step purification procedure, where both chromatography steps were performed in the flow-through mode, enabled us to recover purified HRP glyco-variants for subsequent biochemical characterization. Based thereon, we combined the most suitable mutations to potentially obtain an unglycosylated, active HRP variant suitable for medical applications. Summarizing, we conducted an integrated bioprocess study and present the bioprocess technological and biochemical results for the HRP C1A glyco-variant library.

Results and discussion

Screening procedure

Every transformation into *P. pastoris* CBS7435 Mut^S yielded several dozens of transformants. We randomly picked five transformants per mutation and screened them for cell growth and production of active HRP in shake flasks. With only few exceptions, all the picked transformants produced active HRP; however, on average only three of five showed comparable growth and productivity. PCR analysis confirmed the presence of the target gene in the genome of *P. pastoris*. Although we did not analyze the exact number of gene integration events by real-time polymerase chain reaction, we assumed the integration of a comparable amount of gene copies into the yeast genome due to the fact that we always transformed the same amount of linearized vector DNA into the *P. pastoris* cells (i.e., 2 μg DNA). We had observed such a correlation in a previous study (Krainer et al. 2012). Although we did not check for the exact integration site of the target gene in the host genome, we ascribe the observed differences in protein production during the screening procedure to a fair amount of non-homologous recombination of the transformed HRP C1A gene into the genome of *P. pastoris* (Naatsaari et al. 2012), most likely at different loci in the chromosome, which consequently influences the accessibility of the transcription machinery to the transformed gene (Krainer et al. 2012). In Table I, we compared the growth of the best transformant per mutation as well as the specific activity and thermal stability of the produced HRP C1A glyco-variants. Although diagnostic applications are normally not performed at 60°C, we determined the stability of HRP at this temperature since we observed nice differences for the glyco-variants at this temperature and the assay could be easily performed in the laboratory. Furthermore, we used the thermal stability as a measure for kinetic stability, as also discussed elsewhere (Polizzi et al. 2007; Spadiut et al. 2009). We always included a *P. pastoris* strain expressing the unmutated wild-type (wt) HRP C1A in the screening experiments as control. Although we obtained slightly different results for the wt depending on the screening round, we included the average values for

Table I. Results of screening experiments to identify the most suitable mutation at the single N-glycosylation sites of HRP C1A

Mutation	Results after 96 h of induction					Chosen mutation
	OD_{600}	Cat. activity (U mL^{-1})	Protein content (mg mL^{-1})	Spec. activity (U mg^{-1})	Residual activity after 4 h at 60°C (%)	
wt	25.2	7.5	0.13	48.4	75.0	
N13D	31.8	0.69	0.09	7.29	27.0	→N13D
N13Q	42.3	0.74	0.08	9.10	10.5	
N13S	35.1	–	–	–	–	
N57D	31.4	0.77	0.11	7.00	53	→N57S
N57Q	23.4	2.48	0.13	19.1	43	
N57S	30.3	7.20	0.13	55.4	74	
N158D	32.7	6.11	0.23	26.6	100	→N158D
N158Q	34.1	0.49	0.37	1.32	81.8	
N158S	30.0	0.87	0.13	6.23	90.8	
N186D	36.8	0.10	0.09	1.06	43.1	→N186D
N186Q	47.6	0.07	0.10	0.70	0	
N186S	46.2	0.14	0.09	1.60	36.2	
N198D	21.3	12.1	0.23	53.1	68.1	→N198D
N198Q	19.7	4.31	0.22	20.1	34.1	
N198S	25.1	1.25	0.22	5.84	20.5	
N214D	17.9	5.03	0.11	46.6	46.1	→N214S
N214Q	18.1	4.92	0.13	39.0	41.5	
N214S	14.2	3.17	0.12	25.6	96.0	
N255D	13.6	7.24	0.13	53.9	66.5	→N255D
N255Q	14.2	8.59	0.18	48.3	78.8	
N255S	11.9	5.49	0.15	35.9	74.9	
N268D	13.6	0.56	0.27	2.07	70.6	→N268D
N268Q	12.9	0.40	0.26	1.54	71.0	
N268S	12.6	0.43	0.32	1.34	54.0	

growth, protein production, enzyme activity and thermal stability in Table I for comparison. Based on the determined specific activity and thermal stability, we chose the most suitable mutation at the single N-glycosylation sites. Except for N13S all the produced HRP glyco-variants showed catalytic activity; however, replacement of Asn by Gln never turned out to be the most suitable mutation at any of the eight N-glycosylation sites. Since we did not measure any detectable extracellular protein content for N13S either, we speculate that this mutation caused problems in protein folding and/or secretion, a phenomenon described before (Zhu et al. 1998; Ito, Ishimaru, et al. 2007; Ito, Seri, et al. 2007; Zou et al. 2013). Interestingly, we observed significant differences in enzyme activity and stability depending on the introduced mutation (Table I), and identified three mutations which had been described before, namely at positions N13 and N268 (Asad, Khajeh, et al. 2011) and N255 (Lin et al. 1999), respectively.

Physiological strain characterization in the bioreactor

The different *P. pastoris* strains carrying the respective mutated HRP gene were physiologically characterized in single dynamic batch cultivations in the controlled environment of a bioreactor. After exhaustion of glycerol which was indicated by an increase in the off-gas signal, a 0.5% (v/v) methanol adaptation pulse was applied which was followed by several, subsequent 1.0% (v/v) methanol pulses (an example for this procedure is illustrated for the *P. pastoris* strains expressing the wt enzyme and variant N57S in Figure 1, while illustrations for the other strains are shown in Supplementary data, Figure S1). This dynamic strategy has repeatedly proven to be a very efficient method to physiologically characterize *P. pastoris* strains in a fast and simple manner (Dietzsch et al. 2011a,b; Krainer et al. 2012; Zalai et al. 2012).

In Table II, the determined strain characteristic parameters of all the strains are summarized. Apparently, the introduction of the respective recombinant HRP C1A gene had an impact on the physiology of the *P. pastoris* strains. Although the majority of the strains showed similar maximum specific growth rates on glycerol ($\mu_{max\ gly}$) between 0.24 and 0.28 h^{-1}, the strain carrying the gene HRP C1A N13D showed a nearly 1.3-fold higher $\mu_{max\ gly}$. This effect was even more pronounced with respect to the specific methanol uptake rate during the adaptation pulse ($q_{s\ adapt}$). Surprisingly, when we calculated the average-specific methanol uptake rate during the consecutive 1% (v/v) methanol pulses ($q_{s\ average\ MeOH}$), we observed striking differences between all the strains. One can speculate that the reason for the altered strain physiology lies in the produced HRP glyco-variant itself, since it is known that N-glycosylation can influence protein folding and protein production and thus might affect cell physiology (Zhu et al. 1998; Ito, Ishimaru, et al. 2007; Ito, Seri, et al. 2007; Zou et al. 2013). However, as shown in Table II, the amount of total extracellular protein for each strain at the end of the dynamic batch cultivation was basically the same, indicating that the single mutations did not cause significant problems in protein folding or secretion. We also analyzed the cell-free cultivation broths on SDS gels and obtained the same pattern of protein bands at comparable intensity (graphs not shown). Thus, apparently not the mutated product but rather the locus of the respective introduced gene in the yeast genome had a significant influence on the methanol metabolism of the cells. This influence is also obvious in both yield coefficients (biomass yield,

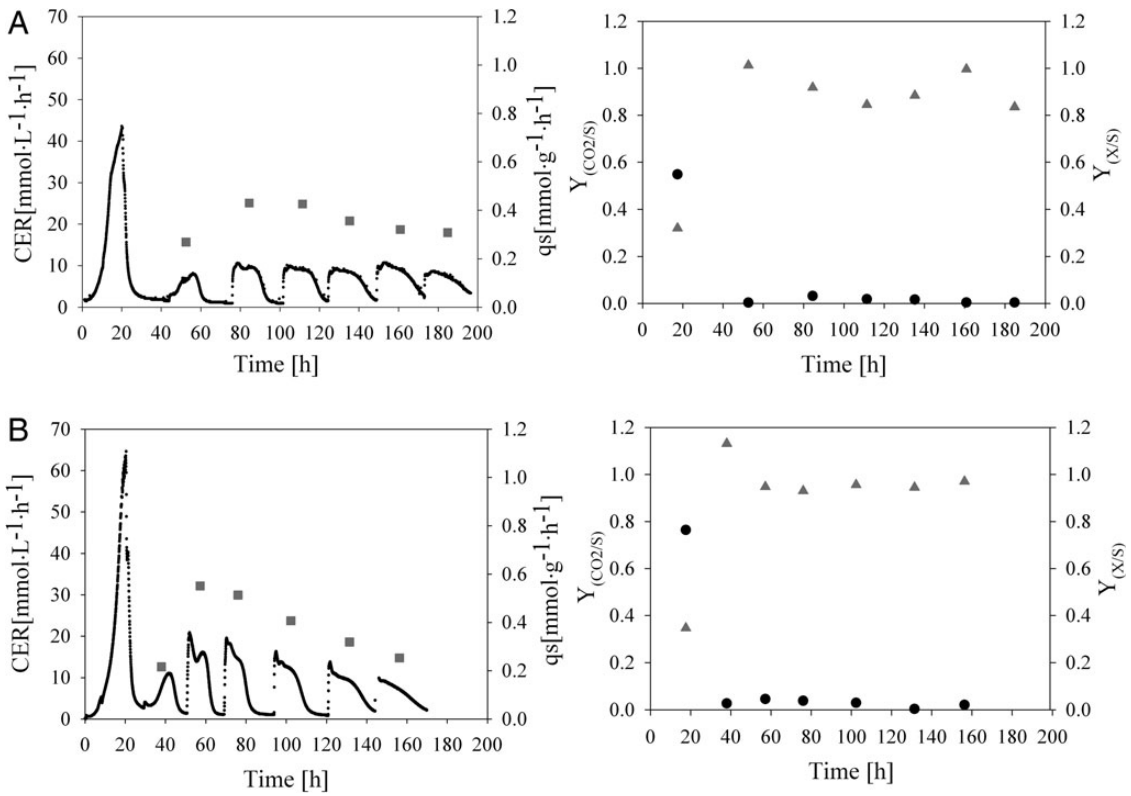

Fig. 1. Batch cultivation of a *P. pastoris* CBS7435 Mut^S strain carrying either the unmutated HRP C1A gene (designated as "wt") or the glyco-variant HRP C1A N57S. A1, batch cultivation with methanol pulses of wt; B1, batch cultivation with methanol pulses of N57S. Solid black line, carbon dioxide evolution rate (CER); gray square, specific substrate uptake rate (q_s). A2, calculated yields of wt; B2, calculated yields of N57S. Gray triangle, carbon dioxide yield ($Y_{CO2/S}$); black dot, biomass yield ($Y_{X/S}$).

Table II. Strain characteristic parameters determined for recombinant *P. pastoris* strains harboring either the wt HRP C1A gene or a glyco-variant thereof and the amount of total extracellular protein at the end of cultivation

Strain	$\mu_{max\ gly}$ (h^{-1})	$\Delta_{time\ adapt}$ (h)	$q_{s\ adapt}$ (mmol g^{-1} h^{-1})	$q_{s\ average\ MeOH}$ (mmol g^{-1} h^{-1})	$Y_{X/S}$ (C_{mol} C_{mol}^{-1})	$Y_{CO2/S}$ (C_{mol} C_{mol}^{-1})	C-balance	Protein (mg mL^{-1})
wt	0.277	11.1	0.269	0.370	0.013	0.92	0.93	0.08
N13D	0.330	8.7	0.317	0.592	0.063	0.88	0.95	0.08
N57S	0.245	12.8	0.216	0.409	0.027	0.95	1.02	0.09
N158D	0.251	13.5	0.211	0.304	0.065	1.00	1.07	0.09
N186D	0.268	13.1	0.211	0.273	0.019	1.00	1.02	0.10
N198D	0.244	8.3	0.292	0.372	0.022	0.90	0.96	0.08
N214S	0.267	14.4	0.219	0.213	0.012	0.95	0.95	0.08
N255D	0.253	8.4	0.291	0.537	0.006	0.96	1.00	0.11
N268D	0.258	14.4	0.253	0.256	0.038	1.00	1.04	0.08

$Y_{X/S}$; carbon dioxide yield, $Y_{CO2/S}$). However, we did not investigate the exact locus of gene integration for the single strains in more detail. Closing C-balances for all cultivations confirm the accuracy of the calculated strain specific parameters. It is remarkable that although we used the same *P. pastoris* strain CBS7435 Mut^S, the same vector and basically the same gene except for single point mutations, we obtained physiologically diverging strains. This actually underlines the importance of a detailed physiological strain characterization using the dynamic method applying methanol pulses, especially if subsequent fed-batch cultivations for protein production are envisioned.

Protein purification

After cultivation, the respective HRP glyco-variant was purified from the cell-free cultivation broth using a previously reported two-step flow-through strategy (Spadiut et al. 2012; Krainer, Pletzenauer, et al. 2013). Total protein content and enzymatic activity were determined in the flow-through and the eluates and the respective recovery yield of HRP activity in percentage (R%) and the purification factor (PF) were calculated for each single purification step (Table III).

After hydrophobic charge induction chromatography (HCIC), we recovered >80% of wt HRP C1A and of most

Table III. Results of the two-step purification approach for HRP C1A applying HCIC and AEC both operated in flow-through mode

Variant	HCIC			AEC			Combined		Spec. activity (U mg^{-1})
	R% total	*R*% FT	PF	*R*% total	*R*% FT	PF	*R*%	PF	
wt	83.6	83.6	1.95	85.9	77.1	3.46	64.5	6.7	248
N13D	91.5	91.5	2.94	85.6	24.5	7.92	22.4	23.3	689
N57S	80.7	80.4	2.70	86.2	70.9	3.32	56.3	9.0	461
N158D	53.8	53.6	1.85	90.1	75.0	5.02	40.2	9.3	167
N186D	86.8	86.8	1.48	91.4	57.1	10.2	49.6	15.1	198
N198D	51.3	51.1	1.30	84.0	50.4	1.89	25.8	2.5	114
N214S	82.4	82.3	1.66	94.4	45.3	4.53	37.3	7.5	113
N255D	94.9	94.9	2.95	96.4	75.4	6.59	71.6	19.4	236
N268D	94.7	94.7	3.43	82.0	74.9	4.21	70.9	14.4	274

enzyme variants except for N158D and N198D. In agreement with our previous observations (Spadiut et al. 2012; Krainer et al. 2013), the whole activity was found in the flow-through. The remaining 5–20% of the enzymes did not elute from the column under the conditions applied, which actually proofs the existence of a variety of enzyme species in the cultivation broth differing in glycosylation and thus a varying degree of interaction with the resin. Interestingly, for glyco-variant N158D and N198D, we only recovered 50% of the enzyme in total, which we also found in the flow-through. Apparently, by mutating these two glycosylation sites and thus reducing the overall amount of surface N-glycosylation, the masking effect thereof was reduced leading to a different HCIC performance for these two enzyme variants. However, compared with the other glycosylation sites we could not identify a particular location of these two sites which could potentially explain this phenomenon (Supplementary data, Figure S2). By HCIC, the wt enzyme was purified 2-fold, whereas the success of purification varied between 1.3- and 3.4-fold for the different glyco-variants highlighting the importance of an integrated bioprocess aspect—already little changes of protein properties, as the degree of surface N-glycosylation, might have a significant impact on following unit operations. The difference in the PF for wt HRP C1A compared with previous studies where we achieved a PF of 7.0 (Krainer, Pletzenauer, et al. 2013) might be explained by the different cultivation strategies. In our previous study, we cultivated *P. pastoris* in shake flasks, where conditions were not controlled and limitations in nutrients and oxygen occurred, which is why cells were more sensitive to cell lysis. Consequently, more contaminating proteins were found in the cell-free cultivation broth. In the present study, we cultivated the different strains in a bioreactor where parameters, such as pH and temperature, were controlled and thus undesired cell lysis was reduced. Consequently, the cell-free cultivation broth contained less contaminating proteins. This is also obvious when looking at the cell-free cultivation broth before purification, which showed a specific activity of only 20 U mg^{-1} from shake flasks (Krainer, Pletzenauer, et al. 2013) but ~40 U mg^{-1} in the present study.

In the subsequent anion exchange chromatography (AEC) step, we recovered >80% of the initially applied HRP for all enzyme variants (Table III). However, the amount of HRP we found in the flow-through vastly differed between the glyco-variants. For the wt enzyme and variants N57S, N158D, N155D and N268D, we found a comparable amount of ~75% of HRP in the flow-through, whereas for variants N13D, N186D, N198D and N214S, the recovery in the flow-through was only 50% or less. For N13D, we even only found 25% of the enzyme in the flow-through, whereas the rest was found in the eluate together with contaminating proteins. However, when we looked at the location of N13 in comparison to the other glycosylation sites we could not identify a particularity which could explain this phenomenon (Supplementary data, Figure S2). This again highlights the importance of the single N-glycosylation sites and the respective surface N-glycosylation for the physicochemical properties of HRP and the applicability of the flow-through chromatography approach. With regard to AEC purification success, we obtained a PF of >3 for the wt enzyme and similar values for N57S, N214S and N268D. Although we only recovered 25% of the initial amount of N13D in the flow-through, this glyco-variant was purified nearly 8-fold. Also N158D, N186D and N255D were purified with great success (5-, 10- and more than 6-fold, respectively), whereas for variant N198D, a PF of only two was determined in the flow-through.

With respect to the overall purification efficiency for the glyco-variant library of HRP C1A using a two-step flow-through approach, we observed vastly different results (Table III). The overall recovery of the initial amount of HRP after the two purification steps varied from only 20% to >70%. Also the obtained total PF varied immensely between 2.5 for variant N198D and >23 for N13D. Remarkably, these vast differences only originated from single point mutations of HRP C1A and consequent changes in surface N-glycosylation. Hence, for some of these variants, such as for N198D, we recommend to adapt the downstream strategy to obtain an enzyme preparation with higher purity.

Biochemical enzyme characterization

After protein purification, the enzyme variants were biochemically characterized. In Table IV, the kinetic constants for the substrates 2,2′-azino-bis(3-ethylbenzothiazoline-6-sulphonic acid) (ABTS) and H_2O_2 are shown. The here presented apparent K_m of 1.60 mM of the wt HRP C1A preparation for ABTS was higher than the previously published K_m values of 0.27 and 0.18 mM for C1A preparations from plant and *E. coli*, respectively (Gilfoyle et al. 1996). However, in previous studies on recombinant HRP C1A from *P. pastoris*, K_m values of 0.68 mM (Morawski et al. 2000) and 1.01 (Krainer, Pletzenauer, et al. 2013) were reported. Apparently, yeast-derived HRP C1A preparations generally have a

Table IV. Kinetic constants of wt HRP C1A and the glyco-variants for the substrates ABTS and H_2O_2 as well as thermal stability

Variant	ABTS			H_2O_2			$\tau_{1/2}$ (min)
	K_m (mM)	V_{max} (U mg^{-1})	V_{max}/K_m (U mg^{-1} mM^{-1})	K_m (mM)	V_{max} (U mg^{-1})	V_{max}/K_m (U mg^{-1} mM^{-1})	
wt	1.60	44.2	27.7	0.003	16.3	5433	20.6
N13D	2.90	47.2	16.3	0.005	14.7	3066	28.9
N57S	2.98	113	38.1	0.004	23.7	5378	38.5
N158D	3.08	16.3	5.30	0.005	51.7	10,342	3.2
N186D	4.24	77.4	18.2	0.004	7.63	2179	18.8
N198D	1.21	14.9	12.3	0.003	19.1	5795	18.5
N214S	3.48	41.1	11.8	0.004	9.36	2531	6.3
N255D	1.72	51.5	29.9	0.005	21.6	4506	11.6
N268D	1.89	32.5	17.2	0.003	10.6	3642	61.9

tendency for a lowered affinity to ABTS compared with preparations from plant and *E. coli*, indicating a crucial role of glycosylation for enzyme activity.

As shown in Table IV, the K_m values of the glyco-variants for ABTS were higher than for the wt, except for variant N198D. Mutating the N-glycosylation sites on the surface of enzyme HRP C1A also affected the reaction rate (Table IV). Summarizing, in terms of catalytic efficiency with ABTS only variants N57S and N255D showed slightly higher or similar values compared with the wt. A similar effect for glyco-variant N255D had already been described elsewhere (Lin et al. 1999). The other glyco-variants were characterized by an up to 5-fold reduced catalytic efficiency. Interestingly, in the work of Asad, Khajeh, et al. (2011) HRP variants N13D and N268D also showed higher catalytic activity compared with the wt. However, Asad et al. used a different reducing substrate as well as different assay conditions, which is why a direct comparison with the present study is not feasible.

We observed similar trends of K_m and V_{max} for the substrate H_2O_2, as the majority of HRP glyco-variants showed a reduced catalytic efficiency compared with the wt enzyme (Table IV). In fact, N57S was the only glyco-variant showing similar or even higher catalytic efficiency with both substrates compared with the wt. The Michaelis–Menten kinetics for the wt enzyme and for variant N57S for both substrates is exemplarily shown in Figure 2, whereas illustrations for the other enzyme variants are shown in the Supplementary data, Figure S3.

To potentially explain the observed effects of the mutations on the surface of the enzyme on the catalytic activity, we determined the distance of the respective N-glycosylation site to the amino acid His170, which is linked to the heme group in the active site (Figure 3). However, we were not able to identify a direct correlation between the distance of the N-glycosylation site to the active site and observed changes in catalytic activity. Only resolving the crystal structures of the single HRP C1A glyco-variants and the subsequent analysis of structure–function relationships could potentially explain the observed effects of the respective mutation on the catalytic behavior.

Finally, we also tested the enzymes for thermal stability, since it is known that mutating N-glycosylation sites on the surface of proteins might affect stability (Asad, Khajeh, et al. 2011). In order to investigate if the protein concentration affects thermal stability, as described elsewhere (Asad, Khajeh, et al. 2011), two different concentrations, i.e., 0.01 and 0.02 mg mL^{-1}, of the wt HRP were tested. In fact, we observed a huge

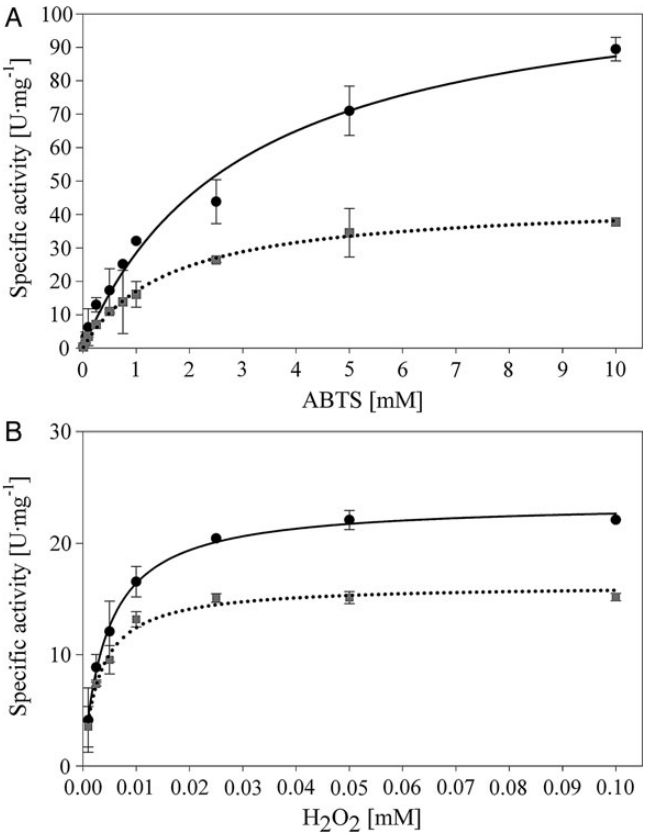

Fig. 2. Michaelis–Menten kinetics of the unmutated wt HRP C1A and the glyco-variant N57S for ABTS and H_2O_2. (**A**) Kinetics for ABTS, (**B**) kinetics for H_2O_2. Black dots, N57S; gray squares, wt.

difference in the half-life time at 60°C, which we determined with 20.6 min for the less concentrated protein solution and with 121 min for the more concentrated one. Consequently, we normalized all the different HRP glyco-variant solutions to a concentration of 0.01 mg mL^{-1} before heat treatment. Interestingly, we found striking differences in the thermal stability of the enzyme glyco-variants (Table IV). For N158D, N214S and N255D stability was significantly reduced, whereas N186D and N198D showed half-life times comparable to the wt. Interestingly, N13D and N57S showed a higher thermal stability and N268D had an even 3-fold higher half-life time ($\tau_{1/2}$)

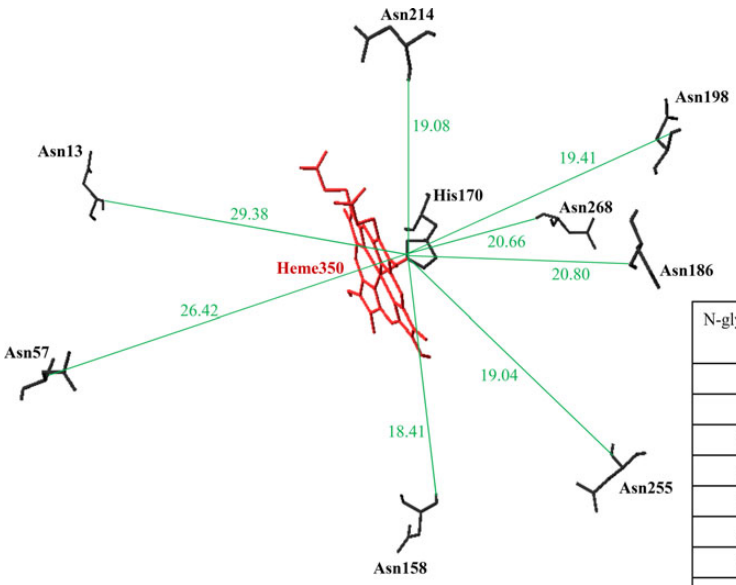

N-glycosylation site	distance to His170 [Å]
N13	29.38
N57	26.42
N158	18.41
N186	20.80
N198	19.41
N214	19.08
N255	19.04
N268	20.66

Fig. 3. Distances of the N-glycosylation sites on the surface of HRP C1A to the heme-binding site His170 in the active site.

than the fully glycosylated enzyme. Comparable observations for variants N13D and N268D were also made by Asad, Khajeh, et al. (2011). The differences between the determined half-life times in this study compared with the study of Asad et al., who determined the stability at 50°C, can be explained by differences in the assay conditions. Whereas Asad, Torabi, et al. (2011) used a 200 mM phosphate buffer, we only used a 50 mM phosphate buffer, which is known to positively affect HRP stability. Summarizing, it is remarkable that mutating glycosylation sites of a protein and thus reducing its overall glycosylation pattern does not only reduce protein stability but might also increase it.

Glycosylation analysis. To prove the absence of surface glycosylation on the respective mutated N-glycosylation site, we exemplarily performed glycosylation analysis for the glyco-variant N57S by digesting the protein with either chymotrypsin or trypsin and subsequently analyzing the peptides by liquid-chromatography mass spectrometry. Furthermore, aliquots of the chymotryptic digest were incubated with PNGase A and released glycans were analyzed by mass spectrometry (Figure 4). The success of mutating Asn57 to a non-glycosylated Ser was confirmed by mass spectrometric analysis of chymotryptic peptides. We clearly see the absence of surface N-glycosylation on N57S (Figure 4).

Combination of mutations

To potentially obtain an enzyme variant without any N-glycosylation, we combined all the eight mutations described in chapter Screening procedure (hereafter called "mutant"). The resulting *P. pastoris* strain was again cultivated in a batch with consecutive methanol pulses for physiological strain characterization (Table V). Again, we observed very different strain characteristic parameters, although we used the same *P. pastoris* strain CBS7435 Mut^S, the same vector and basically the same gene except for eight point mutations. Closing C-balances for both cultivations confirm the accuracy of the calculated strain specific parameters. In contrast to the strain carrying the wt HRP C1A gene, we were not able to detect any HRP activity in the cell-free cultivation broth for the strain carrying the mutated gene. Only after ultrafiltration and 20-fold concentration of the cultivation broth, we were able to measure activity for the mutated HRP C1A glyco-variant. We concentrated the enzyme further and diafiltrated it before we determined the catalytic constants with ABTS and H_2O_2 as well as thermal stability (Table VI). As shown in Table VI, the combination of all eight mutations to obtain a HRP C1A variant without any *N*-glycans resulted in an enzyme variant with extremely reduced catalytic efficiency and thermal stability. Although the affinity towards ABTS basically remained the same, the catalytic activity was reduced nearly 300-fold. The effects for H_2O_2 were even more severe, as K_m was increased >8-fold and V_{max} decreased >100-fold resulting in a nearly 1000-fold reduced catalytic efficiency. As judged by SDS–PAGE analysis, the size of this variant was significantly reduced compared with the glycosylated wt enzyme (figure not shown). However, since catalytic activity and stability were that low, making this variant not useful for medical applications, we did not analyze the surface N-glycosylation of this glyco-variant in more detail.

Summarizing, enzyme engineering describes a valid approach to obtain active HRP C1A variants with a reduced amount of surface N-glycosylation. Although an enzyme variant where all the eight N-glycosylation sites were mutated hardly showed catalytic activity and thus does not describe a meaningful tool for medical applications, the here described glyco-library of HRP C1A describes a very useful basis for further enzyme engineering approaches. Studies, where we only combine up to four mutations, namely N13D, N57S, N255D and N268D, and then express these variants in a *P. pastoris OCH*1 knockout strain (Krainer, Gmeiner, et al. 2013) to obtain a HRP C1A variant useful for targeted cancer treatment are currently ongoing.

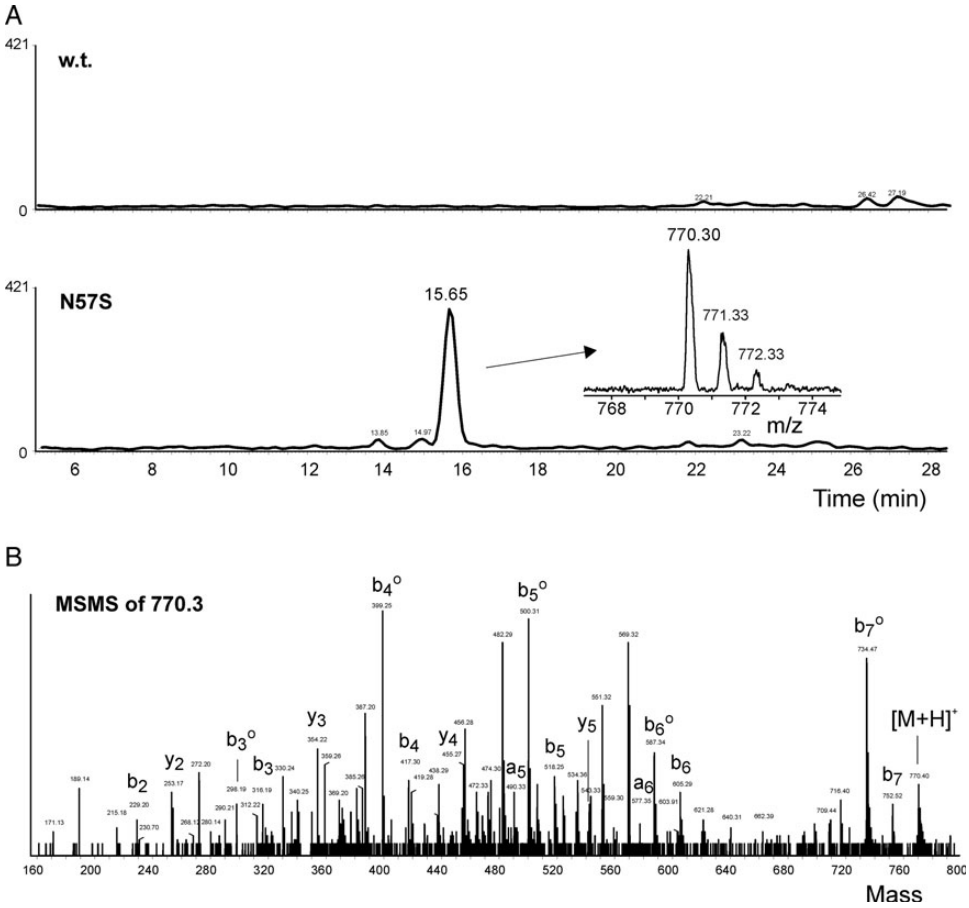

Fig. 4. Verification of the mutated peptide LD^{57}STTSF by MS. (A) The extracted ion chromatograms for the mass of LDSTTSF ([M+H]$^+$ 770.36 Da) in N57S HRP. The mutant exhibited the relevant peak, whose identity was confirmed by CID fragmentation as shown in (B). B-fragments with loss of H_2O are designated as b^o fragments.

Table V. Strain characteristic parameters determined for recombinant *P. pastoris* strains harboring either the wt HRP C1A gene or a variant where all the eight N-glycosylation sites were mutated (mutant)

Strain	$\mu_{max\ gly}$ (h^{-1})	$\Delta_{time\ adapt}$ [h]	$q_{s\ adapt}$ (mmol g^{-1} h^{-1})	$q_{s\ average\ MeOH}$ (mmol g^{-1} h^{-1})	$Y_{X/S}$ (C_{mol} C_{mol}^{-1})	$Y_{CO2/S}$ (C_{mol} C_{mol}^{-1})	C-balance	Protein (mg mL^{-1})
Wt	0.277	11.1	0.269	0.370	0.013	0.92	0.93	0.08
Mutant	0.222	4.7	0.660	0.882	0.153	0.81	0.97	0.10

Table VI. Kinetic constants of wt HRP C1A and the variant where all the eight N-glycosylation sites were mutated (mutant) for the substrates ABTS and H_2O_2 as well as thermal stability

Variant	ABTS			H_2O_2			$\tau_{½}$ (min)
	K_m (mM)	V_{max} (U mg^{-1})	V_{max}/K_m (U mg^{-1} mM^{-1})	K_m (mM)	V_{max} (U mg^{-1})	V_{max}/K_m (U mg^{-1} mM^{-1})	
Wt	1.60	44.2	27.7	0.003	16.3	5433	20.6
Mutant	1.44	0.15	0.10	0.026	0.14	5.38	3.2

Material and methods

Chemicals

Enzymes were purchased from Fermentas GmbH (Vienna, Austria). ABTS diammonium salt was obtained from Sigma–Aldrich Handels GmbH (Vienna, Austria). Difco™ yeast nitrogen base w/o amino acids (YNB), Bacto™ tryptone and Bacto™ yeast extract were obtained from Becton Dickinson and Company (Schwechat, Austria). Zeocin™ was obtained from Invitrogen (Vienna, Austria). D-Biotin was obtained from Fluka Chemia AG (St. Gallen, Switzerland). All other chemicals were purchased from Carl Roth GmbH & Co. KG (Karlsruhe, Germany).

Strain and gene

P. pastoris CBS7435 Mut^S (Dietzsch et al. 2011a,b; Krainer et al. 2012; Zalai et al. 2012; Krainer, Gmeiner, et al. 2013; Spadiut et al. 2013) and vector pPpT4_S harboring the HRP isoenzyme C1A, which was codon-optimized for high-level expression in *P. pastoris* (Krainer et al. 2012), were used in this study. The codon table described in Abad et al. (2010) was applied for codon optimization. Secretion of HRP C1A to the cultivation broth was facilitated by an N-terminally fused prepro-signal sequence of the *S. cerevisiae* alpha-factor.

Site-directed mutagenesis

The eight Asn, representing the glycosylation sites of HRP C1A, were mutated to either Asp, Gln or Ser, which are amino acids providing a certain structural similarity to Asn, by site-directed mutagenesis and subsequent digestion with DpnI (Li and Wilkinson 1997). The mutagenic PCR was performed as: 98°C for 30 s; then 10 cycles of 98°C for 10 s, 57°C for 20 s, 72°C for 1 min—10 cycles of 98°C for 10 s, 60°C for 20 s, 72°C for 1 min—10 cycles of 98°C for 10 s, 63°C for 20 s, 72°C for 1 min; with a final incubation at 72°C for 10 min. Each reaction contained 1× HF buffer (Fermentas), 0.1 µg of plasmid DNA, 2.5 U *Phusion* DNA polymerase (Fermentas), 10 µM of each dNTP and 5 pmol of each primer in a total volume of 50 µL. All primers are listed in Table VII and were purchased from Microsynth (Vienna, Austria).

After PCR, the methylated template DNA was degraded by digestion with 10 U of DpnI at 37°C for at least 3 h. The remaining PCR products were purified using the QIAquick PCR purification kit (QIAGEN, Vienna, Austria) and 5 µL of each purified PCR product were transformed into electro-competent *E. coli* TOP10 F′ cells. The successful introduction of the desired mutation and the absence of further mutations were confirmed by DNA sequencing (Microsynth). Transformation of ~2 µg SwaI-linearized pPpT4_S plasmid DNA harboring the respective mutated HRP C1A gene (Supplementary data, Figure S4) into *P. pastoris* was done as described by Lin-Cereghino et al. (2005). Stable transformants were generated via homologous recombination between the linearized plasmid DNA and genomic yeast DNA. Selection of successfully transformed clones was performed on yeast extract peptone dextrose medium (YPD; 10 g L^{-1} yeast extract, 20 g L^{-1} peptone, 20 g L^{-1} glucose, 20 g L^{-1} agar) supplemented with 100 mg L^{-1} Zeocin.

Screening procedure

Screening of five randomly picked *P. pastoris* transformants per mutation was done in 1000 mL shaking flasks. We also included a *P. pastoris* CBS7435 Mut^S strain carrying the unmutated HRP C1A gene (henceforth designated as "wt") as well as an untransformed *P. pastoris* CBS7435 Mut^S strain as negative control, resulting in a total of 17 shaking flasks per screening experiment. First the clones were cultivated in 10 mL buffered glycerol complex medium supplemented with 100 mg L^{-1} Zeocin (BMGY_Zeo; 10 g L^{-1} yeast extract; 20 g L^{-1} peptone; 3.4 g L^{-1} YNB w/o amino acids and ammonia sulfate, 10 g L^{-1} $(NH_4)_2SO_4$, 400 mg L^{-1} biotin; 1 g L^{-1} glycerol; 0.1 M potassium phosphate buffer, pH 6.0) in 100 mL shaking flasks at 30°C and 230 rpm overnight. The next day the OD_{600} was measured, an appropriate aliquot of the culture was taken, and after centrifugation the cells were resuspended in selective buffered methanol complex medium supplemented with 100 mg L^{-1} Zeocin (BMMY_Zeo; 10 g L^{-1} yeast extract; 20 g L^{-1} peptone; 3.4 g L^{-1} YNB w/o amino acids and ammonia sulfate, 10 g L^{-1} $(NH_4)_2SO_4$, 400 mg L^{-1} biotin; 0.5% methanol; 0.1 M potassium phosphate buffer, pH 6.0) to an OD_{600} of 1.0. The cells were again cultivated at 30°C and 230 rpm. Every day, 1% (v/v) methanol was pulsed to the culture and a 1 mL sample was taken, analyzed for optical density (OD_{600}), catalytic activity and protein content. The catalytic activity of HRP was measured using an ABTS assay in a CuBiAn XC enzymatic robot (Bielefeld, Germany). Ten microliters of sample were mixed with 140 µL 1 mM ABTS solution (50 mM KH_2PO_4, pH 6.5). The reaction mixture was incubated at 37°C for 5 min before the reaction was started by the addition of 20 µL 0.078% H_2O_2 (v/v). Changes in absorbance at 415 nm were measured for 80 s and rates were calculated. The standard curve was prepared using a commercially available HRP preparation (Type VI-A; Sigma–Aldrich) in the range from 0.02 to 2.0 U mL^{-1}. Protein concentrations were determined at 595 nm by the Bradford assay using the Sigma–Aldrich Protein Assay Kit with bovine serum albumin as standard in the range of 0.2–1.2 mg mL^{-1}.

After 96 h of induction, the HRP glyco-variants in the cell-free supernatants were tested for thermal stability. Therefore, aliquots of 1 mL were incubated in a waterbath at 60°C for up to 4 h, before the samples were centrifuged (14,000 rpm; 10 min)

Table VII. Oligonucleotide primers to mutate the eight Asn residues of the enzyme HRP C1A, which act as N-glycosylation sites, to either Asp, Gln or Ser

N-site	Name	Sequence (5′→3′)
N13	N13D_fwd	AAC TCT TGT CCT *GAT* GTG TCC AAC ATC
	N13Q_fwd	AAC TCT TGT CCT *CAG* GTG TCC AAC ATC
	N13S_fwd	AAC TCT TGT CCT *AGT* GTG TCC AAC ATC
	N13_rev	AGG ACA AGA GTT ATC GTA GAA GGT TGG AGT
N57	N57D_fwd	TCC ATC TTG CTG GAC *GAC* ACT ACC TC
	N57Q_fwd	TCC ATC TTG CTG GAC *CAG* ACT ACC TC
	N57S_fwd	TCC ATC TTG CTG GAC *AGC* ACT ACC TC
	N57_rev	GTC CAG CAA GAT GGA AGC ATC ACA ACC
N158	N158D_fwd	C AGA AAC GTT GGT CTT *GAC* AGA TCA TCC
	N158Q_fwd	C AGA AAC GTT GGT CTT *CAG* AGA TCA TCC
	N158S_fwd	C AGA AAC GTT GGT CTT *AGC* AGA TCA TCC
	N158_rev	AAG ACC AAC GTT TCT GAA AGA GTC TTT CAA TTG
N186	N186D_fwd	ATG GAT CGT CTG TAC *GAC* TTC TCT AAC AC
	N186Q_fwd	ATG GAT CGT CTG TAC *CAG* TTC TCT AAC AC
	N186S_fwd	ATG GAT CGT CTG TAC *AGC* TTC TCT AAC AC
	N186_rev	GTA CAG ACG ATC CAT GAT GAA TCT ACA TTG GTT
N198	N198D_fwd	CCA GAT CCT ACT CTG *GAC* ACC ACT TAC
	N198Q_fwd	CCA GAT CCT ACT CTG *CAG* ACC ACT TAC
	N198S_fwd	CCA GAT CCT ACT CTG *AGC* ACC ACT TAC
	N198_rev	CAG AGT AGG ATC TGG CAA ACC GG
N214	N214D_fwd	CCA CTT AAC GGA *GAC* CTG TCT GC
	N214Q_fwd	CCA CTT AAC GGA *CAG* CTG TCT GC
	N214S_fwd	CCA CTT AAC GGA *AGC* CTG TCT GC
	N214_rev	TCC GTT AAG TGG GCA CAA ACC TC
N255	N255D_fwd	TTG TTC TCC TCT CCT *GAC* GCT ACT GAT
	N255Q_fwd	TTG TTC TCC TCT CCT *CAG* GCT ACT GAT
	N255S_fwd	TTG TTC TCC TCT CCT *AGC* GCT ACT GAT
	N255_rev	AGG AGA GGA GAA CAA CTC CTG GTC
N268	N268D_fwd	G AGA TCC TTC GCA *GAC* TCC ACT CAA
	N268Q_fwd	G AGA TCC TTC GCA *CAG* TCC ACT CAA
	N268S_fwd	G AGA TCC TTC GCA *AGC* TCC ACT CAA
	N268_rev	TGC GAA GGA TCT CAC CAA TGG AAT G

The mutation sites are depicted in italics.

and the supernatants were analyzed for remaining HRP activity. These values were then compared with the initial activity before heat treatment. Based on activity and stability measurements, the most suitable mutation at a respective N-glycosylation site was chosen and the corresponding *P. pastoris* strain was physiologically characterized in the bioreactor. Before bioreactor cultivation, the presence of the correctly mutated HRP gene in the respective *P. pastoris* transformant was verified by colony PCR using the primers AOX_fwd (5′-ACTCCAACCTTCTACGATAACTC-3′) and AOX_rev (5′-ACTGTGTCATGTGCTGACC-3′) and subsequent sequencing (Microsynth).

Strain characterization in the bioreactor

Culture media. Precultures were done in yeast nitrogen base medium with 100 mg L^{-1} Zeocin (YNBM_Zeo; 3.4 g L^{-1} YNB w/o amino acids and ammonia sulfate, 10 g L^{-1} $(NH_4)_2SO_4$, 400 mg L^{-1} biotin, 20 g L^{-1} glucose, 0.1 M potassium phosphate buffer, pH 6.0). Batch cultivations were performed in basal salt medium (26.7 mL L^{-1} 85% phosphoric acid, 1.17 g L^{-1} $CaSO_4{\cdot}2H_2O$, 18.2 g L^{-1} K_2SO_4, 14.9 g L^{-1} $MgSO_4{\cdot}7H_2O$, 4.13 g L^{-1} KOH, 40 g L^{-1} glycerol, 0.2 mL L^{-1} Antifoam Struktol J650, 4.35 mL L^{-1} PTM1, NH_4OH as N-source). Trace element solution (PTM1) was made of 6.0 g L^{-1} $CuSO_4{\cdot}5H_2O$, 0.08 g L^{-1} NaI, 3.0 g L^{-1} $MnSO_4{\cdot}H_2O$, 0.2 g L^{-1} $Na_2MoO_4{\cdot}2H_2O$, 0.02 g L^{-1} H_3BO_3, 0.5 g L^{-1} $CoCl_2$, 20.0 g L^{-1} $ZnCl_2$, 65.0 g L^{-1} $FeSO_4{\cdot}7H_2O$, 0.2 g L^{-1} biotin, 5 mL L^{-1} H_2SO_4. Induction was carried out in presence of 1 mM Δ-aminolevulinic acid. The concentration of the base NH_4OH was determined by titration with 0.25 M potassium hydrogen phthalate.

Experimental procedure

Preculture. Frozen stocks (−80°C) were cultivated in 100 mL YNBM in 1000 mL shake flasks at 30°C and 230 rpm. The grown preculture was transferred aseptically to the respective culture vessel. The inoculation volume was 10% of the final starting volume.

Batch cultivation. Batch cultivations were carried out in either a 3 L or a 5 L working volume glass bioreactor (Infors, Bottmingen, Switzerland). Basal salt medium was sterilized in the bioreactor and pH was adjusted to pH 5.0 by using concentrated NH_4OH solution after autoclaving. Sterile filtered trace elements were transferred to the reactor aseptically. Dissolved oxygen (dO_2) was measured with a sterilizable dO_2 electrode (Visiferm™, Hamilton, Bonaduz, Switzerland). The pH was measured with a sterilizable electrode (Easyferm™, Hamilton, Bonaduz, Switzerland) and maintained constant with a PID controller using NH_4OH solution (1–2 M). Base consumption was determined gravimetrically. Cultivation temperature was set to 30°C and agitation was fixed to 1200 rpm. The culture was aerated with 1.0 vvm dried air and off-gas of the culture was measured by using an infrared cell for CO_2 and a paramagnetic cell for O_2 concentration (Servomax, Hyderabad, India). Temperature, pH, dO_2, agitation as well as CO_2 and O_2 in the off-gas were measured online and logged in a process information management system (Lucullus, Biospectra, Schlieren, Switzerland). After the complete consumption of the substrate glycerol, indicated by an increase of dO_2 and a drop in off-gas activity, the first methanol pulse of a final concentration of 0.5% (v/v) was conducted with methanol supplemented with 12 mL L^{-1} PTM1. Following pulses were performed with 1% methanol/PTM1 (v/v) (Figure 2). For each pulse, two samples were taken to determine the concentrations of substrate and product, as well as dry cell weight to calculate specific rates and yields.

Analysis of growth and expression parameters

Dry cell weight was determined by centrifugation of 5 mL culture broth (5000 rpm, 4°C, 10 min) in a laboratory centrifuge (Sigma 4K15, rotor 11156), washing the pellet twice with 5 mL deionized water and subsequent drying at 105°C to a constant weight.

Substrate concentrations

Concentrations of methanol were determined in cell-free samples by HPLC (Vienna, Austria) equipped with an ion-exchange column (Supelcogel C-610H Sigma–Aldrich) and a refractive index detector (Agilent Technologies). The mobile phase was 0.1% H_3PO_4 with a constant flow rate of 0.5 mL min^{-1} and the system was run isocratic at 30°C. Calibration was done by measuring standard points in the range from 0.1 to 10 g L^{-1} methanol. Measurements of biomass, product and substrate concentration were executed in duplicates.

Protein purification

After bioreactor cultivation, the cell-free cultivation broth was diafiltrated for subsequent HCIC using a Centramate 500S TFF system (PALL, Vienna, Austria) with a 10 kDa MWCO membrane. The buffer was HCIC-A (500 mM NaCl, 20 mM NaOAc, pH 6.0) and the protein solution was concentrated to a final volume of 40–50 mL. All further steps of concentration and buffer change were performed using Amicon Ultra-15 Centrifugal Filter Units with 10 kDa MWCO (Merck Millipore; Vienna, Austria). The HCIC resin MEP HyperCel™ was obtained from PALL and HCIC was performed in flow-through mode: a column containing 25 mL of MEP HyperCel™ resin was equilibrated with at least 4 column volumes (CV) of buffer HCIC-A. Forty to 50 mL concentrated HRP solution in HCIC-A were loaded onto the column which was then washed with at least 5 CV of HCIC-A at a flow rate of 55 cm h^{-1}. Then a step elution to 100% buffer HCIC-B (1.0 M NaCl, 20 mM NaOAc, pH 8.0) was performed. After elution, the column was washed with 5 CV 0.8 M NaOH before it was stored in EtOH 20%, 1.0 M NaCl. During all the different steps, fractions of 10 mL were collected and analyzed for protein content and catalytic activity.

HCIC flow-through fractions showing HRP activity were pooled, concentrated and rebuffered in AEC-A (50 mM Tris–HCl, pH 8.0) for subsequent AEC using an 8 mL CIM®-DEAE monolithic column (Krainer, Pletzenauer, et al. 2013) (BIAseparations, Ajdovščina, Slovenia). The column was equilibrated with 5 CV of AEC-A at a flow rate of 16.8 cm h^{-1}. Diafiltrated post-HCIC pools were subsequently loaded onto the AEC column at an average linear flow rate of 16.8 cm h^{-1} before a post-load wash with 5 CV of AEC-A was performed. Elution was performed in a single step from 0 to 100% AEC-B (50 mM Tris–HCl, 1.0 M NaCl, pH 8.0). The column was washed with 5 CV of a 1 M NaOH/1 M NaCl solution at an average linear flow rate of 33.6 cm h^{-1} for column recovery, before the column was stored in 20% EtOH.

The efficiency of each purification step was evaluated by determining the PF and the recovery yield of HRP activity in percentage (R%). PF and R% were calculated by Eqs (1) and (2) (Krainer, Pletzenauer, et al. 2013). The suffixes "pre" and "post" indicate the respective values before and after a purification step.

$$\mathrm{PF} = \frac{\text{specific activity}_{\text{post}}}{\text{specific activity}_{\text{pre}}}, \quad (1)$$

$$R\% = 100 \times \frac{\text{volumetric activity}_{\text{post}} \times \text{volume}_{\text{post}}}{\text{volumetric activity}_{\text{pre}} \times \text{volume}_{\text{pre}}}. \quad (2)$$

Finally, the pooled active fractions after AEC were diafiltrated in 50 mM potassium phosphate buffer, pH 6.5, and concentrated to a volume of ~1.5 mL for the subsequent biochemical characterization.

Biochemical enzyme characterization

Biochemical characterization of the purified HRP glyco-variants included the determination of the basic kinetic parameters K_m and V_{max} for the two substrates H_2O_2 and ABTS in a spectrophotometer UV-1601 from Shimadzu (Korneuburg, Austria). The reaction mixture with a final volume of 1.0 mL contained 20 µL of HRP glyco-variant, 50 mM potassium phosphate buffer, pH 6.5, and either varying concentrations of ABTS (0.01–10 mM) and a saturating concentration of H_2O_2 of 1.0 mM or varying concentrations of H_2O_2 (0.001–1.0 mM) and a saturating concentration of ABTS of 10.0 mM, respectively. The increase in absorption was followed at 420 nm at 30°C for 180 s. Absorption curves were recorded with a software program (UVPC Optional Kinetics software, Shimadzu). The maximum reaction rate (V_{max}) and the Michaelis constant (K_m) were calculated with the Sigma Plot software (Version 11.0; Systat Software Inc.).

The thermal stability of individual HRP glyco-variants was tested at 60°C. The residual activity towards ABTS was measured after 1, 5, 10, 15, 30, 45, 60, 90 and 120 min of incubation at 60°C in a water bath. Protein concentrations were normalized to 0.01 mg mL to limit possible effects of the different protein concentrations on thermal stability (Asad, Khajeh, et al. 2011) and to obtain comparability. Residual activities were plotted versus the incubation time and the half-life times of thermal inactivation at 60°C ($\tau_{½}$) were calculated using Eq. (3):

$$\tau_{1/2} = \frac{\ln 2}{k_{in}}, \quad (3)$$

k_{in} rate of inactivation (slope of the logarithmic residual activity).

Glycosylation analysis. Purified HRP sample was buffered in 0.1 M NH_4HCO_3 and reduced with dithiothreitol (5 mM) for 45 min at 56°C and alkylated using iodoacetamide (25 mM) at room temperature for 30 min. The protein was precipitated with 4 volumes of acetone for 45 min at −20°C, dried in a vacuum centrifuge and resuspended in 0.1 M NH_4HCO_3 buffer to yield a protein concentration of ~1 µg µL^{-1}. Digests were performed overnight with either chymotrypsin or trypsin (Promega, Mannheim, Germany) at 37°C at an enzyme-to-substrate ratio of 1:50 (w/w). The digested peptides were analyzed by liquid-chromatography mass spectrometry as follows: 1 µg of sample was loaded on a BioBasic-18 column (150 × 0.32 mm; 5 µm; Thermo Scientific, Vienna, Austria) and eluted with a gradient from 1 to 60% acetonitrile in 0.3% formic acid buffered to pH 3.0 at flow rate of 6 µL min. Eluted peptides were analyzed on an Ultima Global Q-TOF mass spectrometer (Waters, Manchester, UK) operated in positive-ion mode, which was previously calibrated with a cesium iodide standard in the range of 400–1800 *m/z*. Additionally, the peptide harboring the site N57S within the mutated HRP variant was subjected to collision-induced dissociation MS-MS with Argon as collision gas. Data were manually evaluated and deconvoluted using the Software MassLynx V4.00.00 (Waters).

An aliquot of the chymotryptic digest was heat inactivated and then incubated with 0.03 mU PNGase A (Proglycan, Vienna, Austria) in 50 mM citrate buffer, pH 5.5. Glycans were purified using porous graphitic carbon cartridges (Thermo Scientific) as described (Pabst et al. 2012). Glycans were analyzed by mass spectrometry as described in chapter Glycosylation analysis for peptides with the sole divergence of using a 100 × 0.32 mm hypercarb column (Thermo Scientific) and 1 h gradient from 1 to 50% acetonitrile.

Supplementary Data

Supplementary data for this article are available online at http://glycob.oxfordjournals.org/.

Funding

The authors are very grateful to the Austrian Science Fund FWF: project P24861-B19 for financial support. Funding to pay the Open Access publication charges for this article was provided by the Austrian Science Fund FWF (project P24861-B19).

Acknowledgements

We further thank the company BIA separations (Slovenia) for providing the tube monolithic columns.

Conflict of interest statement

None declared.

Abbreviations

ABTS, 2,2′-azino-bis(3-ethylbenzothiazoline-6-sulphonic acid); AEC, anion exchange chromatography; CV, column volumes; HCIC, hydrophobic charge induction chromatography; HRP, horseradish peroxidase; H_2O_2, hydrogen peroxide; mutant, HRP C1A, where all eight N-glycosylation sites were mutated; PF, purification factor; R%, recovery yield of HRP activity in percentage; $\tau_{½}$, thermal half-life time; wt, wild type; X, any amino acid but proline; $Y_{X/S}$, biomass yield (C-mol·C-mol^{-1}); $Y_{CO2/S}$, carbon dioxide yield (C-mol·C-mol^{-1}).

References

Abad S, Nahalka J, Bergler G, Arnold SA, Speight R, Fotheringham I, Nidetzky B, Glieder A. 2010. Stepwise engineering of a Pichia pastoris D-amino acid oxidase whole cell catalyst. *Microb Cell Fact*. 9:24.

Asad S, Khajeh K, Ghaemi N. 2011. Investigating the structural and functional effects of mutating Asn glycosylation sites of horseradish peroxidase to Asp. *Appl Biochem Biotechnol*. 164:454–463.

Asad S, Torabi SF, Fathi-Roudsari M, Ghaemi N, Khajeh K. 2011. Phosphate buffer effects on thermal stability and H_2O_2-resistance of horseradish peroxidase. *Int J Biol Macromol*. 48:566–570.

Carlsson GH, Nicholls P, Svistunenko D, Berglund GI, Hajdu J. 2005. Complexes of horseradish peroxidase with formate, acetate, and carbon monoxide. *Biochemistry* 44:635–642.

Choi BK, Bobrowicz P, Davidson RC, Hamilton SR, Kung DH, Li HJ, Miele RG, Nett JH, Wildt S, Gerngross TU. 2003. Use of combinatorial genetic libraries to humanize N-linked glycosylation in the yeast Pichia pastoris. *Proc Natl Acad Sci USA*. 100:5022–5027.

Dietzsch C, Spadiut O, Herwig C. 2011a. A dynamic method based on the specific substrate uptake rate to set up a feeding strategy for Pichia pastoris. *Microb Cell Fact*. 10:14.

Dietzsch C, Spadiut O, Herwig C. 2011b. A fast approach to determine a fed batch feeding profile for recombinant Pichia pastoris strains. *Microb Cell Fact*. 10:85.

Dotsikas Y, Loukas YL. 2012. Improved performance of antigen-HRP conjugate-based immunoassays after the addition of anti-HRP antibody and application of a liposomal chemiluminescence marker. *Anal Sci*. 28:753–757.

Dunford HB. 1999. *Heme Peroxidases*. New York: Wiley-VCH.

Ehlers MRW, Chen YNP, Riordan JF. 1992. The unique N-terminal sequence of testis angiotensin-converting enzyme is heavily O-glycosylated and unessential for activity or stability. *Biochem Biophys Res Commun*. 183:199–205.

Folkes LK, Wardman P. 2001. Oxidative activation of indole-3-acetic acids to cytotoxic species – a potential new role for plant auxins in cancer therapy. *Biochem Pharmacol*. 61:129–136.

Gajhede M, Schuller DJ, Henriksen A, Smith AT, Poulos TL. 1997. Crystal structure of horseradish peroxidase C at 2.15 angstrom resolution. *Nat Struct Biol*. 4:1032–1038.

Gilfoyle DJ, Rodriguez-Lopez JN, Smith AT. 1996. Probing the aromatic-donor-binding site of horseradish peroxidase using site-directed mutagenesis and the suicide substrate phenylhydrazine. *Eur J Biochem*. 236:714–722.

Hamilton SR, Bobrowicz P, Bobrowicz B, Davidson RC, Li HJ, Mitchell T, Nett JH, Rausch S, Stadheim TA, Wischnewski H, et al. 2003. Production of complex human glycoproteins in yeast. *Science*. 301:1244–1246.

Hamilton SR, Gerngross TU. 2007. Glycosylation engineering in yeast: The advent of fully humanized yeast. *Curr Opin Biotechnol*. 18:387–392.

Huang RP. 2001. Detection of multiple proteins in an antibody-based protein microarray system. *J Immunol Methods*. 255:1–13.

Ito K, Ishimaru T, Kimura F, Matsudomi N. 2007. Importance of N-glycosylation positioning for secretion and folding of ovalbumin. *Biochem Biophys Res Commun*. 361:725–731.

Ito K, Seri A, Kimura F, Matsudomi N. 2007. Site-specific glycosylation at Asn-292 in ovalbumin is essential to efficient secretion in yeast. *J Biochem*. 141:193–199.

Jermyn MA. 1952. Horseradish peroxidase. *Nature*. 169:488–489.

Jermyn MA, Thomas R. 1954. Multiple components in horse-radish peroxidase. *Biochem J*. 56:631–639.

Kang LX, Chen XM, Fu L, Ma LX. 2012. Recombinant expression of chitosanase from Bacillus subtilis HD145 in Pichia pastoris. *Carbohydr Res*. 352:37–43.

Krainer FW, Dietzsch C, Hajek T, Herwig C, Spadiut O, Glieder A. 2012. Recombinant protein expression in Pichia pastoris strains with an engineered methanol utilization pathway. *Microb Cell Fact*. 11:22.

Krainer FW, Gmeiner C, Neutsch L, Windwarder M, Pletzenauer R, Herwig C, Altmann F, Glieder A, Spadiut O. 2013. Knockout of an endogenous mannosyltransferase increases the homogeneity of glycoproteins produced in Pichia pastoris. *Sci Rep*. 3:3279.

Krainer FW, Pletzenauer R, Rossetti L, Herwig C, Glieder A, Spadiut O. 2013. Purification and basic biochemical characterization of 19 recombinant plant peroxidase isoenzymes produced in Pichia pastoris. *Protein Expr Purif*. 95C:104–112.

Krieg R, Halbhuber KJ. 2003. Recent advances in catalytic peroxidase histochemistry. *Cell Mol Biol*. 49:547–563.

Lavery CB, MacInnis MC, MacDonald MJ, Williams JB, Spencer CA, Burke AA, Irwin DJG, D'Cunha GB. 2010. Purification of peroxidase from horseradish (Armoracia rusticana) roots. *J Agric Food Chem*. 58:8471–8476.

Li S, Wilkinson MF. 1997. Site-directed mutagenesis: A two-step method using PCR and DpnI. *Biotechniques*. 4:588–590.

Lin-Cereghino J, Wong WW, Xiong S, Giang W, Luong LT, Vu J, Johnson SD, Lin-Cereghino GP. 2005. Condensed protocol for competent cell preparation and transformation of the methylotrophic yeast Pichia pastoris. *Biotechniques*. 38:44–48.

Lin Z, Thorsen T, Arnold FH. 1999. Functional expression of horseradish peroxidase in E. coli by directed evolution. *Biotechnol Prog*. 15:467–471.

Morawski B, Lin ZL, Cirino PC, Joo H, Bandara G, Arnold FH. 2000. Functional expression of horseradish peroxidase in Saccharomyces cerevisiae and Pichia pastoris. *Protein Eng*. 13:377–384.

Naatsaari L, Mistlberger B, Ruth C, Hajek T, Hartner FS, Glieder A. 2012. Deletion of the Pichia pastoris KU70 homologue facilitates platform strain generation for gene expression and synthetic biology. *PLoS ONE*. 7:e39720.

Narhi LO, Arakawa T, Aoki KH, Elmore R, Rohde MF, Boone T, Strickland TW. 1991. The effect of carbohydrate on the structure and stability of erythropoietin. *J Biol Chem*. 266:23022–23026.

Pabst M, Grass J, Toegel S, Liebminger E, Strasser R, Altmann F. 2012. Isomeric analysis of oligomannosidic N-glycans and their dolichol-linked precursors. *Glycobiology*. 22:389–399.

Palmgren B, Jin Z, Jiao Y, Kostyszyn B, Olivius P. 2011. Horseradish peroxidase dye tracing and embryonic statoacoustic ganglion cell transplantation in the rat auditory nerve trunk. *Brain Res*. 1377:41–49.

Polizzi KM, Bommarius AS, Broering JM, Chaparro-Riggers JF. 2007. Stability of biocatalysts. *Curr Opin Chem Biol*. 11:220–225.

Powell LM, Pain RH. 1992. Effects of glycosylation on the folding and stability of human, recombinant and cleaved alpha-1-antitrypsin. *J Mol Biol*. 224:241–252.

Romero MI, Romero MA, Smith GM. 1999. Visualization of axonally transported horseradish peroxidase using enhanced immunocytochemical detection: A direct comparison with the tetramethylbenzidine method. *J Histochem Cytochem*. 47:265–272.

Sainz-Pastor N, Tolner B, Huhalov A, Kogelberg H, Lee YC, Zhu D, Begent RH, Chester KA. 2006. Deglycosylation to obtain stable and homogeneous Pichia pastoris-expressed N-A1 domains of carcinoembryonic antigen. *Int J Biol Macromol*. 39:141–150.

Shannon LM, Kay E, Lew JY. 1966. Peroxidase isozymes from horseradish roots. I. Isolation and physical properties. *J Biol Chem*. 241:2166–2172.

Smith AT, Santama N, Dacey S, Edwards M, Bray RC, Thorneley RNF, Burke JF. 1990. Expression of a synthetic gene for horseradish peroxidase-C in Escherichia coli and folding and activation of the recombinant enzyme with Ca^{2+} and heme. *J Biol Chem*. 265:13335–13343.

Spadiut O, Herwig C. 2013. Production and purification of the multifunctional enzyme horseradish peroxidase: A review. *Pharm Bioproc*. 1:283–295.

Spadiut O, Leitner C, Salaheddin C, Varga B, Vertessy BG, Tan TC, Divne C, Haltrich D. 2009. Improving thermostability and catalytic activity of pyranose 2-oxidase from Trametes multicolor by rational and semi-rational design. *FEBS J*. 276:776–792.

Spadiut O, Rossetti L, Dietzsch C, Herwig C. 2012. Purification of a recombinant plant peroxidase produced in Pichia pastoris by a simple 2-step strategy. *Protein Expr Purif*. 86:89–97.

Spadiut O, Zalai D, Dietzsch C, Herwig C. 2013. Quantitative comparison of dynamic physiological feeding profiles for recombinant protein production with Pichia pastoris. *Bioprocess Biosyst Eng*. doi: 10.1007/s00449-013-1087-z.

Tams JW, Welinder KG. 1995. Mild chemical deglycosylation of horseradish-peroxidase yields a fully active, homogeneous enzyme. *Anal Biochem*. 228:48–55.

Tams JW, Welinder KG. 1998. Glycosylation and thermodynamic versus kinetic stability of horseradish peroxidase. *FEBS Lett*. 421:234–236.

Veitch NC. 2004. Horseradish peroxidase: A modern view of a classic enzyme. *Phytochemistry*. 65:249–259.

Veitch NC, Smith AT. 2001. Horseradish peroxidase. *Adv Inorg Chem*. 51:107–162.

Vervecken W, Kaigorodov V, Callewaert N, Geysens S, De Vusser K, Contreras R. 2004. In vivo synthesis of mammalian-like, hybrid-type N-glycans in Pichia pastoris. *Appl Environ Microbiol*. 70:2639–2646.

Wang CQ, Eufemi M, Turano C, Giartosio A. 1996. Influence of the carbohydrate moiety on the stability of glycoproteins. *Biochemistry*. 35:7299–7307.

Wardman P. 2002. Indole-3-acetic acids and horseradish peroxidase: A new prodrug/enzyme combination for targeted cancer therapy. *Curr Pharm Des*. 8:1363–1374.

Zalai D, Dietzsch C, Herwig C, Spadiut O. 2012. A dynamic fed batch strategy for a Pichia pastoris mixed feed system to increase process understanding. *Biotechnol Prog*. doi:10.1002/btpr.1551

Zhu A, Wang ZK, Beavis R. 1998. Structural studies of alpha-N-acetylgalactosaminidase: Effect of glycosylation on the level of expression, secretion efficiency, and enzyme activity. *Arch Biochem Biophys*. 352:1–8.

Zou S, Huang S, Kaleem I, Li C. 2013. N-Glycosylation enhances functional and structural stability of recombinant beta-glucuronidase expressed in Pichia pastoris. *J Biotechnol*. 164:75–81.